EPR study of defects in neutron-irradiated silicon: Quenched-in alignment under ⟨110⟩-uniaxial stress*

Young-Hoon Lee and James W. Corbett
Department of Physics, State University of New York at Albany, Albany, New York 12222
(Received 4 February 1974)

The stress effect in an EPR study is first treated rigorously in terms of the piezospectroscopic tensor, taking account of the local symmetry of a defect. It is found that the degree of alignment ($n_\perp/n_\parallel$) provides incisive information on the structure of a defect; in general, a nonplanar vacancy cluster results in $n_\perp/n_\parallel < 1.0$ and a {110}-planar vacancy chain gives rise to $n_\perp/n_\parallel > 1.0$. We reanalyze the results on the Si-$P1$ and Si-$P3$ spectra. Based on the quenched-in alignment under ⟨110⟩ uniaxial stress, we confirm the assignment on the Si-$P1$ and the Si-$P3$ spectra to a negative charge state of nonplanar pentavacancy cluster and to the neutral charge state (spin 1) of the {110}-planar tetravacancy chain, respectively. Tentative models of the Si-$A3$ as a tetravacancy cluster and the Si-$A4$ spectra as a {110}-planar trivacancy chain are discussed.

I. INTRODUCTION

The response of EPR spectra to an externally applied uniaxial stress provides important information on the microscopic structure of defects. This technique has been utilized by Watkins and Corbett[1-3] to confirm the atomic configuration in the vicinity of radiation-induced defects in silicon. As an external stress is applied, it disturbs the normal cubic symmetry of the crystal and the 12 equivalent sites of the {110}-symmetric defect,[4] for instance, are no longer in equal energy states. In thermal equilibrium, therefore, the defects with different orientations with respect to the stress axis no longer yield lines of equal intensity in the EPR spectrum. It is well known in silicon[2] that defect reorientation among the equivalent sites under uniaxial stress may arise from either electronic or atomic motion.

Since we are dealing with a number of vacancy-associated defects in the silicon crystal, we define, for convenience, the new nomenclature to describe the following vacancy clusters: a "{110}-planar vacancy chain" consists of a number of vacancies in a {110}-plane, making a "saw-tooth" shaped vacancy string along the ⟨110⟩ axis, such as the trivacancy center; a "{111}-planar vacancy cluster" is one in which vacancies are all confined in the two closest {111} planes formed by the "chair" structure; a "nonplanar vacancy cluster" is one that belongs to neither of the first two groups.

In this report, we discuss the stress effects in {110}-symmetric defects, particularly emphasizing the results obtained in the EPR spectra in neutron-irradiated silicon. The stress experiment is carried out at high temperature in order to observe the quenched-in alignment; i.e., the sample was heated to a high temperature (140–150 °C) under the ⟨110⟩-axial stress (~ 2000 kg/cm^2) and then was cooled quickly to room temperature with stress on. After releasing the pressure, the sample was placed in the 35-GHz cavity for measurement. Details of the experiment will be described later for each spectrum we have studied.

In Sec. II, we establish the basic formulation for analyzing the stress effect in terms of the Kaplyanskii's piezospectroscopic tensor,[5] which provides the complete group-theoretic characterization of the defects. This formulation is compared to the earlier, less complete analysis. The present analysis takes account of the local symmetry around a defect which may be deduced very easily from the number of the EPR central lines in an arbitrary direction of the magnetic field. Each component in the piezospectroscopic tensor is also discussed from a physical viewpoint, in light of the well-understood defect centers such as the phosphorus-plus-vacancy pair ($G8$)[2] and the oxygen-plus-vacancy pair ($B1$)[1] which are reanalyzed in terms of the new analysis. In Sec. III, the stress results obtained in the several spectra in the neutron-irradiated silicon are presented in terms of the new parameters defined in Sec. II, and the defect models of $P1$, $P3$, $A3$, and $A4$ spectra will be discussed, based on the quenched-in alignment. Section IV is a summary.

II. STRESS ALIGNMENT-FOUNDATION

We consider a compressional stress applied along a ⟨110⟩-axis as indicated in Fig. 1 (a). The number of degeneracies among the equivalent defect sites with respect to the stress axis, as tabulated by Kaplyanskii,[5] depends only on the local symmetry of a given defect. In the case of the C_{1h}-symmetric defects ("monoclinic I" in the Kaplyanskii nomenclature), for example, there are four different groups of equivalent defects, energetically different from each other, under the ⟨110⟩-uniaxial stress, as shown in Fig. 1 (b). The order of energy levels depends upon the microscopic configuration of the defect. (We will discuss

this point later in Sec. II B.) In Fig. 1 (b), we simply present the actual situation of the $G8$ spectrum arising from the phosphorus-plus-vacancy pair, a C_{1h}-symmetric defect. We will follow the earlier designation[2] of the defects in C_{1h} symmetry; e.g., ad represents a defect orientation whose g_1 axis is closest to the ⟨111⟩ axis d, and the g_3-axis closest to a.

As the ⟨110⟩ external stress is applied, the defect energy level Δ_0, originally twelve-fold degenerate, will split into four distinct levels, Δ_{ad}, Δ_{ac}, Δ_{bd}, and Δ_{bc}, where ad, ac, etc., refer to particular orientations of the defects. To first order, the energy splittings are linearly proportional to the applied stress; that is,

$$\Delta = \vec{\vec{B}} \cdot \vec{\vec{\epsilon}} = \vec{\vec{B}} \cdot \vec{\vec{S}} \cdot \vec{\vec{\sigma}} \quad , \tag{1}$$

where $\vec{\vec{\sigma}}$ and $\vec{\vec{\epsilon}}$ represent, respectively, the stress tensor and the strain tensor of the second rank. $\vec{\vec{B}}$ refers to the piezospectroscopic tensor characteristic of the defect in question and $\vec{\vec{S}}$ is the elasticity tensor (of fourth rank), which can be derived for the host lattice in terms of the coordinate system (x, y, z) given in Fig. 1 (a)[6]:

$$\vec{\vec{S}} = \begin{pmatrix} \frac{1}{4}(2s_{11}+2s_{12}+s_{44}) & \frac{1}{4}(2s_{11}+2s_{12}-s_{44}) & s_{12} & 0 & 0 & 0 \\ \frac{1}{4}(2s_{11}+2s_{12}-s_{44}) & \frac{1}{4}(2s_{11}+2s_{12}+s_{44}) & s_{12} & 0 & 0 & 0 \\ s_{12} & s_{12} & s_{11} & 0 & 0 & 0 \\ 0 & 0 & 0 & s_{44} & 0 & 0 \\ 0 & 0 & 0 & 0 & s_{44} & 0 \\ 0 & 0 & 0 & 0 & 0 & 2(s_{11}-s_{12}) \end{pmatrix} .$$

The piezospectroscopic tensor $\vec{\vec{B}}$ in the same coordinate system can be easily calculated from the Kaplyanskii A tensor,[5] and using Eq. (1), we can derive the energy splittings due to the ⟨110⟩ compression, $-p$, by considering six distinct ⟨110⟩ axes in the cubic lattice. The results are as follows, for three different symmetries frequently encountered in the EPR spectra:

(i) C_{1h} symmetry (monoclinic I):

$$\vec{\vec{B}} = \begin{pmatrix} B_1 & 0 & 0 \\ 0 & B_2 & B_4 \\ 0 & B_4 & B_3 \end{pmatrix} ,$$

$$\Delta_{bc} = -\tfrac{1}{4}p[B_1(2s_{11}+2s_{12}+s_{44}) + B_2(2s_{11}+2s_{12}-s_{44}) + 4B_3 s_{12}] \quad , \tag{2a}$$

$$\Delta_{bd} = -\tfrac{1}{4}p[(B_1+B_2)(s_{11}+3s_{12}) + 2B_3(s_{11}+s_{12}) - \sqrt{2}\, B_4 s_{44}] \quad , \tag{2b}$$

$$\Delta_{ac} = -\tfrac{1}{4}p[(B_1+B_2)(s_{11}+3s_{12}) + 2B_3(s_{11}+s_{12}) + \sqrt{2}\, B_4 s_{44}] \quad , \tag{2c}$$

$$\Delta_{ad} = -\tfrac{1}{4}p[B_1(2s_{11}+2s_{12}-s_{44}) + B_2(2s_{11}+2s_{12}+s_{44}) + 4B_3 s_{12}] \quad . \tag{2d}$$

The degeneracy is $d(ad) = d(bc) = 2$ and $d(ac) = d(bd) = 4$.

(ii) C_{2v} symmetry (rhombic I):

$$\vec{\vec{B}} = \begin{pmatrix} B_1 & 0 & 0 \\ 0 & B_2 & 0 \\ 0 & 0 & B_3 \end{pmatrix} ,$$

$$\Delta_{bc} = -\tfrac{1}{4}p[B_1(2s_{11}+2s_{12}+s_{44}) + B_2(2s_{11}+2s_{12}-s_{44}) + 4B_3 s_{12}] \quad , \tag{3a}$$

$$\Delta_{bd} = \Delta_{ac} = -\tfrac{1}{4}p[(B_1+B_2)(s_{11}+3s_{12}) + 2B_3(s_{11}+s_{12})] \quad , \tag{3b}$$

$$\Delta_{ad} = -\tfrac{1}{4}p[B_1(2s_{11}+2s_{12}-s_{44}) + B_2(2s_{11}+2s_{12}+s_{44}) + 4B_3 s_{12}] \quad . \tag{3c}$$

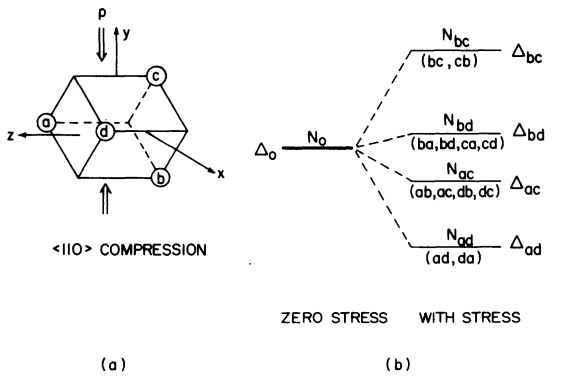

FIG. 1. (a) Four ⟨111⟩ directions are designated by a, b, c, and d with respect to the ⟨110⟩-uniaxial compression p applied along the Y axis. (b) Owing to the ⟨110⟩ stress, twelvefold orientational degeneracy (energy level Δ_0 and concentration N_0) in the C_{1h} defects is split into the four subgroups Δ_{ad}, Δ_{ac}, Δ_{bd}, and Δ_{bc}, where $N_0 = 2(N_{ad}+N_{bc}) + 4(N_{ac}+N_{bd})$. The order of the energy levels is uniquely determined by the electronic structure of a defect and the actual situation of the $G8$ spectrum is simply shown.

The degeneracy is $d(ad)=d(bc)=2$ and $d(bd)=8$.

(iii) C_{3v} symmetry (trigonal):

$$\vec{\vec{B}}=\begin{pmatrix} B_1 & 0 & \frac{1}{2}\sqrt{2}\,(B_1-B_2) \\ 0 & B_2 & 0 \\ \frac{1}{2}\sqrt{2}\,(B_1-B_2) & 0 & \frac{1}{2}\sqrt{2}\,(B_1+B_2) \end{pmatrix},$$

$$\Delta_{bc}=-\tfrac{1}{4}p[B_1(2s_{11}+4s_{12}+s_{44}) +B_2(2s_{11}+4s_{12}-s_{44})] \quad , \tag{4a}$$

$$\Delta_{ad}=-\tfrac{1}{4}p[B_1(2s_{11}+4s_{12}-s_{44}) +B_2(2s_{11}+4s_{12}+s_{44})] \quad . \tag{4b}$$

The degeneracy is $d(ad)=d(bc)=6$.

Experimentally, correlation of each energy level with a particular defect site is made (i) by comparing the relative intensity of EPR signal lines at $\vec{H}\parallel\langle 110\rangle$ with the degree of degeneracy, d, of the energy levels and (ii) by choosing the coordinate system [(x, y, z) in Fig. 1 (a)] in such a way that B_2 (the y axis) is always parallel to the g_2 axis in the g tensor.

Consider first the C_{1h} symmetry assuming that the reorientation of the defect axis takes place by either atomic or electronic motion so as to repopulate the defects between the sublevels Δ_{ad}, Δ_{bc}, Δ_{ac}, and Δ_{bd} in the deformed crystal. In thermal equilibrium, then, the defect concentration at each level, N_{ac}, N_{ad}, N_{bc}, and N_{bd}, should be proportional to the Boltzmann factor, and the relative population, which can be measured experimentally from the intensity of the central lines, will be, at a given temperature T,

$$N_{ad}/N_{bc}=e^{-T_\alpha/T} \quad , \tag{5a}$$

$$N_{ad}/N_{ac}=e^{-T_\beta/T} \quad , \tag{5b}$$

$$N_{ac}/N_{bd}=e^{-T_\gamma/T} \quad , \tag{5c}$$

with

$$kT_\alpha=\Delta_{ad}-\Delta_{bc}=(\epsilon_{ad}-\epsilon_{bc})(B_1-B_2) \tag{6a}$$

$$kT_\beta=\Delta_{ad}-\Delta_{ac}=(\epsilon_{ad}-\epsilon_{ac})B_1+(\epsilon_{bc}-\epsilon_{ac})B_2 +\tfrac{1}{2}p(s_{11}-s_{12})B_3+\tfrac{1}{4}\sqrt{2}\,ps_{44}B_4 \quad , \tag{6b}$$

$$kT_\gamma=\Delta_{ac}-\Delta_{bd}=-\tfrac{1}{2}\sqrt{2}\,ps_{44}B_4 \quad , \tag{6c}$$

where we used the earlier notation of the strain components [Eqs. (27) in Ref. (1)]; i.e.,

$$\epsilon_{ad}=-\tfrac{1}{4}p(2s_{11}+2s_{12}-s_{44}) \quad ,$$

$$\epsilon_{bc}=-\tfrac{1}{4}p(2s_{11}+2s_{12}+s_{44}) \quad ,$$

$$\epsilon_{ac}=-\tfrac{1}{4}p(s_{11}+3s_{12}) \quad .$$

The uniaxial-stress experiments give three parameters [the T_i's in Eqs. (6)] which are not sufficient to determine the four B_i's. Complete analysis would be possible if the hydrostatic pressure change in energy, given by TrB, is determined by experiment or theory. We note, however, that B_4 is determined directly by Eq. (6c).

A similar situation exists for defects with C_{2v} symmetry. Following the same arguments we easily arrive at

$$kT_\alpha=(\epsilon_{ad}-\epsilon_{bc})(B_1-B_2) \quad , \tag{7a}$$

$$kT_\beta=(\epsilon_{ad}-\epsilon_{ac})B_1+(\epsilon_{bc}-\epsilon_{ac})B_2 +\tfrac{1}{2}p(s_{11}-s_{12})B_3 \quad . \tag{7b}$$

The corresponding $T_\gamma=0$ because Δ_{ac} and Δ_{bd} are degenerate. The uniaxial-stress experiments yield two parameters [the T_i's in Eqs. (7)] which are related to three parameters (the B_i's), and again additional information is required to determine the B_i's.

We can, however, apply the equations to experiment. Consider the oxygen-plus-vacancy pair,[1] which has C_{2v} symmetry. The earlier analysis[1] was in terms of two parameters, $M_{\text{Si-Si}}$ and $N_{\text{Si-O-Si}}$, which because we have chosen the B_2 axis parallel to g_2 are equal to B_1 and B_2, respectively. That analysis, by using just two parameters, is the same as assuming $B_3=0$. If we put B_3 equal zero in Eqs. (7), we obtain the identical equations used earlier, i.e., Eqs. (26c) and (26d) of Ref. 1. As shown in Fig. 2, the parameter B_3 arises from the strain effect along the Z axis for the defect sites whose {110} reflection planes are tilted 60° from the ⟨110⟩ stress axis. Viewed more physically, B_3 can be described as the energy change per unit strain when two Si atoms, a

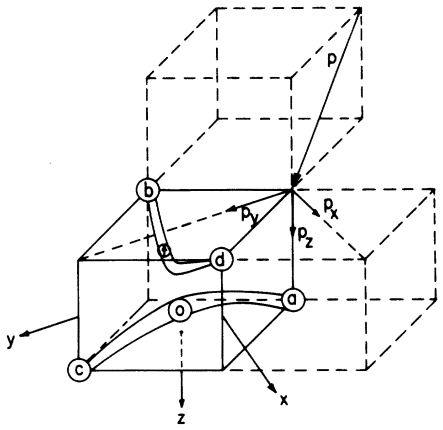

FIG. 2. ⟨110⟩-stress effect of the oxygen-plus-vacancy pair (a C_{2v}-symmetric defect) in the defect site bd; the compression p is neither the Si-Si nor Si-O-Si bond direction. Its P_x component corresponds to the B_1 parameter in the Si-Si bond and the P_y component to B_2 in the Si-O-Si bond. There exists an additional effect of B_3 due to the P_z component along the Z axis, which forces a pair of the bonding atoms to move away from each other.

and c forming a Si-O-Si bond (or b and d forming a Si-Si pair bond) move away from each other along the Y axis (or X axis) due to the Z component of the applied stress. The previous analysis of the $B1$ center[1] ignored B_3 so as to determine the important parameters, B_1 and B_2, from Eqs. (7). Based on that analysis, the hydrostatic pressure term is

$$\mathrm{Tr}\, B = B_1 + B_2 + B_3 = 33.2 \text{ eV/(unit strain)} \quad ,$$

which seems too large since the sign of B_3 should be opposite to that of both B_1 and B_2, and since the normal cubic lattice of silicon gives $\mathrm{Tr}\, B = \frac{1}{2}(s_{11} + 2s_{12})^{-1} \Delta V \sim 1$ eV/(unit strain) for a volume change $\Delta V = 1$ Å^3. From this latter result we argue that the value

$$B_1 + B_2 + B_3 = 0 \qquad (8)$$

would be appropriate as a first-order approximation, in the situation of our experiments, where the external uniaxial stress is normally of the order of 2000 kg/cm^2.

Using Eqs. (7a), (7b), and (8), with $T_\alpha = -8$ °K, $T_\beta = -84$ °K, and $p = 879$ kg/cm^2 given in Table IV of Ref. 1, we reestimate the parameters:

$$B_1 (= M) = 4.8 \text{ eV/(unit strain)} \quad ,$$

$$B_2 (= N) = 6.1 \text{ eV/(unit strain)} \quad ,$$

$$B_3 = -10.9 \text{ eV/(unit strain)}$$

for the oxygen-plus-vacancy pair. Here, the elastic-constant values $s_{11} = 7.68 \times 10^{-13}$, $s_{12} = -2.14 \times 10^{-13}$, and $s_{44} = 12.56 \times 10^{-13}$ (in cm^2/dyn) are used. The present values of B_1 and B_2 are roughly a factor of 3 smaller than the previous results obtained under the assumption that $B_3 = 0$. We note that the new estimates are rather close to a typical value of the deformation potential (~3 eV) of silicon, and the fact that B_3 is approximately twice as large as B_1 or B_2 seems reasonable, because both pair bonds, Si-Si and Si-O-Si, should contribute to the B_3 component. It should be emphasized, however, that the validity of both approximations (i.e., $B_3 = 0$ or $\mathrm{Tr}B = 0$) remains in question until the hydrostatic contribution is known.

We can similarly reanalyze some of the C_{1h} defects. Elkin and Watkins[7] pointed out that the levels Δ_{ac} and Δ_{bd} were nondegenerate, but the analysis was done in terms of only one parameter ($B_2 = M_{\mathrm{Si-Si}}$); if $B_1 = B_3 = B_4 = 0$, Eq. (6b) becomes equal to Eq. (22) in Ref. 2. Since the alignment data for the $G6$, $G7$, and $G23$ spectra (all of which have C_{1h} symmetry) that is available in the original papers[3,7] are not sufficient to obtain their B_4 component, we reanalyzed only the $G8$ and $G24$ spectra. As we can clearly see in Fig. 15 of Ref. 2 and Fig. 11 of Ref. 7, however, B_4 cannot be zero in both $G8$ and $G24$ spectra; i.e., the defect concentration of the ac site is different from that of the bd site. Using Eq. (6c), B_4 can be directly obtained without the assumption of Eq. (8); $B_4 = 4.1$ eV/(unit strain) for the $G8$ spectrum and 8.3 eV/(unit strain) for the $G24$ spectrum. (These estimates are based on the alignment data in Fig. 15 of Ref. 2 and in Fig. 11 of Ref. 7.)

From the definition of B_4 in the B matrix, we may interpret B_4 as the change in the defect energy caused by a shear stress on the Z plane with the Y component (or on the Y plane with the Z component) of the applied stress (see Fig. 3), which exists only at the defect sites whose {110}-reflection plane is neither parallel nor perpendicular to the ⟨110⟩-stress axis. Since $B_4 = 0$ in the C_{2v} symmetry, the magnitude of B_4 reflects the distortion of the C_{1h} defects from C_{2v} symmetry. Viewed more physically, for example, in the phosphorus-plus-vacancy pair shown in Fig. 3, distortion of the plane in which the pair-bonding orbital lies would cause the energy change B_4 of that orbital. The pair bond, formed by two atoms, c and d, may not be originally in a normal {110} plane (the X plane in Fig. 3), but may be slightly off from the {110} plane toward the position of the phosphorus atom due to the Coulomb repulsion between the dangling bond and the pair-bond orbitals. By pulling (or pushing) the plane of the pair bond from (or to) the {110} plane, the effect of B_4 will be different depending on the position of the phosphorus atom with respect to the stress axis; the situation where the P atom is located at the a site (the defect ac) must be different from the case where the P atom is at the c site (the defect ca), even though they have the same pair bond (bd). The same argument can be generally applied to all of the C_{1h} defects, where the pair bonds are formed in the ⟨110⟩ direction perpendicular to the reflection plane.

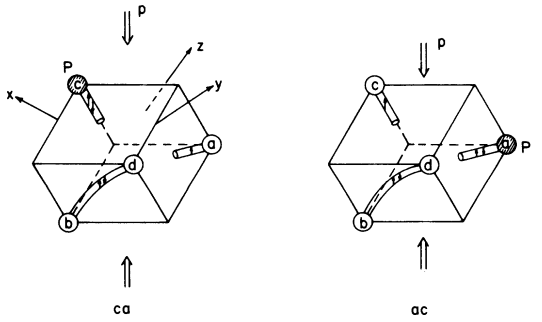

FIG. 3. Phosphorus-plus-vacancy pair at the defect sites ca and ac; although both defects have the same Si-Si pair bond between the b and d atoms, the stress alignment is different, depending on the position of the dangling bond where the unpaired electron is localized. This difference is due to the B_4 parameter. [See their energy levels in Fig. 1(b)].

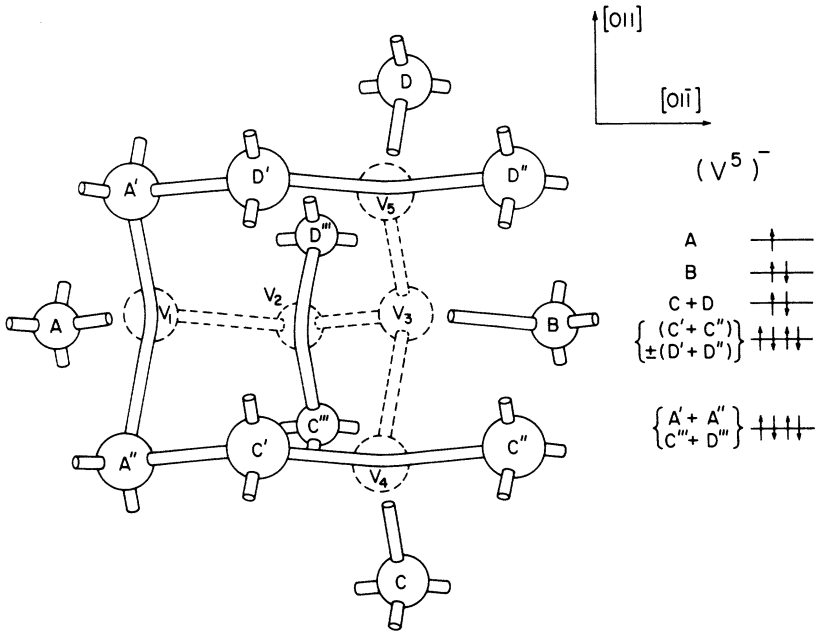

FIG. 4. Defect structure of a nonplanar pentavacancy cluster (the $P1$ center); vacancies are shown with dotted lines.

In Sec III, we describe our experimental results in the nonplanar pentavacancy cluster (the $P1$ spectrum)[8,9] and in the planar tetravacancy chain (the $P3$ spectrum)[10,11] both dominant defects in heavily damaged silicon.

III. EXPERIMENTAL RESULTS AND DISCUSSIONS

A. Si-$P1$ spectrum

The $P1$ spectrum is known to be one of the important paramagnetic centers in either neutron- or ion-bombarded silicon. On the basis of detailed studies of the Si^{29} hyperfine structure and of the temperature dependence in the g tensor, we[9] have recently attributed the spectrum to a negative charge state of a nonplanar pentavacancy cluster. The microscopic structure of the defect is shown in Fig. 4, where three vacancies (V_1, V_2, and V_3) are aligned in a row along the $[01\bar{1}]$ axis and two more vacancies (V_4 and V_5) sit at both sides of the end one (V_3) along the [011] axis so that the {110}-reflection plane is retained.

Preferential alignment of the defect is achieved by applying a ⟨110⟩-compressional stress at an elevated temperature. An unannealed sample [intrinsic floating zone with total neutron fluence (nvt) of 10^{18} n/cm^2, in which the $P1$ spectrum was initially absent, was heated in an electric oven for 2 h under 2200-kg/cm^2 compression, until the sample temperature increased to 225 °C. When the temperature reached 225 °C, it was kept constant for 30 min and then the sample was cooled to room temperature in 5 min with stress on. After releasing the pressure, the sample was removed from the oven and placed in the 35-GHz cavity for room-temperature measurements. The results are shown in Fig. 5; the spectra were taken with the magnetic field parallel to the ⟨110⟩ axis (a) with zero stress and (b) with the quenched-in alignment after the pressure was applied. Here, we also indicate the other spectra,[12] $A3$, $A4$, $A6$, and $A9$, which appeared along with the $P1$ spectrum; the $P1$ central lines are labeled in terms of the corresponding defect sites.

It is observed that a quenched-in alignment has taken place favoring the defect whose g_2 axis is perpendicular to the stress axis; i.e., $N_{bc} > N_{bd} > N_{ac} > N_{ad}$, contrary to the previous observation in the divacancy center,[3] where $N_{ad} > N_{ac} > N_{bd} > N_{bc}$. In other words, the order of the energy levels in Fig. 1 (b) is reversed in the case of the $P1$ spectrum. We note that all the ⟨110⟩-symmetric defects which have been studied thus far reveal the same feature of alignment as the divacancy center. (We will see one example later in Sec. III C.) In order to rule out the possibility of there being anisotropic creation of the defect in the deformed crystal by the reverse annealing effect (the annealing study showed[12] that the $P1$ spectrum undergoes reverse annealing at a temperature below ~260 °C), the same experiment was carried out with a different procedure; the sample was first annealed for 1 h without stress, and when the temperature reached 150 °C, a ⟨110⟩ compression (2000 kg/cm^2) was applied for 30 min; the sample was quenched in 5 min down to room temperature. Also, the same procedure was followed at 280 °C with 2000 kg/cm^2. Both cases provided the same sense of alignment described before; i.e., N_{bc}

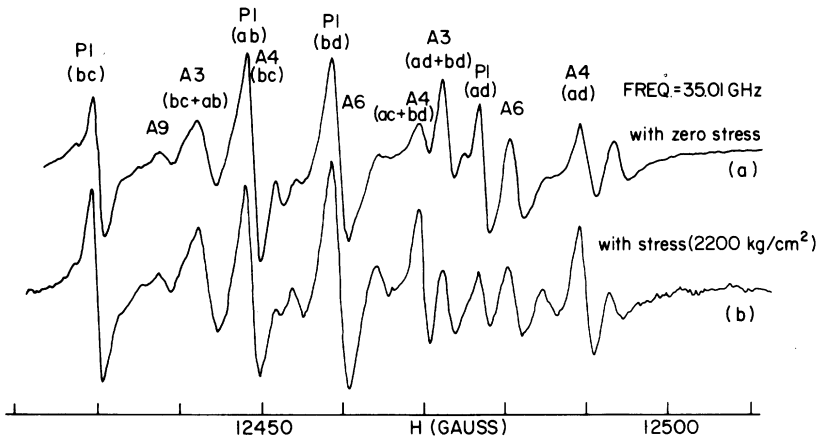

FIG. 5. EPR spectra with $\vec{H} \parallel \langle 110 \rangle$ and $T = 300$ °K: (a) at the 225 °C anneal with no stress on and (b) after the quenched-in alignment was achieved at 225 °C with the $\langle 110 \rangle$-uniaxial stress (2200 kg/cm^2). Each signal line is designated by the spectral name and the corresponding defect site. In the $P1$ spectrum, $N_{bc} > N_{ad}$ and $N_{bd} > N_{ab}$.

$> N_{bd} > N_{ac} > N_{ad}$. We conclude, therefore, that the preferential alignment seen in the $P1$ spectrum, is caused by reorientation of the defect sites through atomic motion.

The degree of alignment, defined as[2]

$$\frac{n_\perp}{n_\parallel} = \frac{N_{ad}+N_{ab}+N_{ac}}{N_{bc}+N_{ba}+N_{bd}} ,$$

is given in Table I with those for the other centers which appeared at the same time. For comparison, we also present the defects studied by Watkins and Corbett. Using Eqs. (5), (6), and (8), we estimate the strain energy in terms of the parameters B_1, B_2, B_3, and B_4 as presented in Table II, where the values in parentheses are the ones calculated on the assumption that $B_3 = 0$.

The striking difference of the $P1$ center from the rest of the centers in Table II is that the signs of B_2 and B_4 are reversed from the corresponding parameters of others. Watkins and Corbett argued that the energy change in the pair-bonding orbitals plays a major role in preferential alignments of the defects. This means that the alignment of the $P1$ center must be strongly controlled by the pair bonds aligned in the direction ($[01\bar{1}]$ axis in Fig. 4) perpendicular to the g_2 axis and parallel to the $\langle 110 \rangle$ axis closest to the g_1 axis. Those pair bonds so oriented could not exist if the defect is a $\{110\}$-planar vacancy chain along the $\langle 110 \rangle$ axis, like the divacancy center, but *do* exist in the case of a nonplanar or $\{111\}$-planar vacancy cluster. We argue, therefore, that the sign of B_4 (or the degree of alignment, $n_\perp/n_\parallel$) provides very decisive information on whether a defect in question is a vacancy cluster or a $\{110\}$-planar chain.

In light of our model of the $P1$ center shown in Fig. 4, the two pair bonds (D', D'') and (C', C'') are formed in the direction parallel to the $[01\bar{1}]$ axis, and perpendicular to it, there are two more pair bonds (A', A'') and (C''', D''') along the [011] axis (the g_2 axis). Thus, the number of the pair bonds is equal in both directions. Interpretation of the stress alignment could become easier if we constructed a new model, the septevacancy cluster, by putting two more vacancies at the atomic sites C and D so that a number of the pair bonds in the $[01\bar{1}]$ axis is larger than in the other direction ([011] axis). But as we reasoned in Ref. 9, the possibility of a septevacancy cluster can be excluded on the grounds that (i) the Si^{29} hyperfine structure from the second-neighbor sites suggests six or seven equivalent sites and that (ii) the concentration of the $P1$ defect is comparable to that of the tetravacancy center. Furthermore, the above argument is purely based on the presumption that all the pair bonds are energetically equivalent. This equivalence is not obviously true in the situation of our model for the $P1$ center. The stress results suggest that the pair bonds (A', A'') and (C''', D''') are coupled much more strongly than (C', C'') and (D', D''). Thus, the atoms C', C'', D', and D'' may be easily distorted by the external stress and the stress effect must be influ-

TABLE I. Degree of alignment under a $\langle 110 \rangle$ compression at a high temperature. Reference numbers are in parentheses.

Spectrum	Temp. (°C)	Stress (kg/cm^2)	Period (min)	$\frac{n_\perp}{n_\parallel}$
Si-$P1$	225	2200	30	0.72
Si-$P3$	140	2250	30	1.37
Si-$A2$	225	2200	30	0.71
Si-$A3$	225	2200	30	0.65
Si-$A4$	225	2200	30	1.40
Si-$A5$	140	2250	30	2.0
Si-$A9$	225	2200	30	1.38
Si-$G6$ (3)	160	1870	60	1.50
Si-$G7$ (3)	160	1870	60	1.50
Si-$G8$ (2)	25	1830	60	1.75
Si-$G9$ (15)	190	1700	15	1.33
Si-$G23$ (7)	110	3200	15	1.51
Si-$G24$ (7)	110	3200	15	1.76

TABLE II. Piezospectroscopic tensor of C_{1h}-symmetric defects. [The parameters are determined under the ⟨110⟩-uniaxial compression at high temperatures in units of eV/ (unit strain) and the values in parentheses are obtained on the presumption $B_3 = 0$.]

Spectrum	Stress (kg/cm^2)	Temp. (°C)	B_1	B_2	B_3	B_4	ϕ[c] (deg.)
Si-$P1$	2000	280	14.5	−13.0	−1.5	−15.8	21.0
			(+15.9)	(−11.7)	(0)	(−15.8)	
Si-$P3$	2250	140	−1.6	9.7	−8.1	4.1	1.6
			(6.5)	(17.8)	(0)	(4.1)	
Si-$G8$[a]	1828.4	25	2.8	7.1	−9.9	4.1	4.0
			(4.2)	(8.5)	(0)	(4.1)	
Si-$G24$[b]	3200	110	−4.7	5.2	−0.5	8.3	−17.6
			(−4.1)	(5.8)	(0)	(8.3)	

[a]Results are based on Fig. 15 of Ref. 2.
[b]Results are based on Fig. 11 in Ref. 4.
[c]ϕ is the distortion angle of the g tensor measured from the ⟨111⟩ axis.

enced by the pair bonds (C', C'') and (D', D'') along the $[01\bar{1}]$ axis. Namely, the defect reorientation may take place due to the motion of the two vacancies V_4 and V_5. Therefore, the parameter B_1, the defect energy change made by pulling the two atoms D' and D'' (also C' and C'') closer together, should be the dominant factor. We note that B_1 of the {110}-planar vacancy chain ($G8$, $G24$, and $P3$ in Table II) is either very small or negative compared with that of the $P1$ center. The situation is reversed in the parameter B_2 associated with the orbital energy in the pair bonds parallel to the g_2 axis. The negative sign of B_3 for the centers in Table II is physically reasonable in light of the {110} symmetry of the defects, because B_3 is due to the strain effect, which always forces the pair-bonding atoms away from each other so as to decrease the strain energy. The parameter B_4, a measure of the distortion in the pair-bonding plane, depends on which direction the pair bond favors the distortion from the {110}-plane. We note that the absolute value of B_4 is proportional to the distortion angle of the g tensor, as measured from the ⟨111⟩ axis, closest to the g_1 axis and given in the last column of Table II. When the g_1 axis is closer to the ⟨111⟩ axis, B_4 becomes comparable to the deformation potential. We conclude that the stress results provide strong support for our model of the $P1$ center being due to a pentavacancy cluster.

B. Si-$P3$

The $P3$ spectrum is one of the spin-1 centers identified first by Jung and Newell[10] in high-fluence ($\sim 10^{18}$ n/cm^2) neutron-bombarded silicon. It was later also found in ion-implanted silicon.[13] It can be observed prior to heat treatment and disappears at 170 °C. Brower[11] has attributed the spectrum to the {110}-planar tetravacancy chain along the ⟨110⟩ axis, as shown in Fig. 6. When four vacancies are formed in a row along the ⟨110⟩ direction, those dangling bonds having reflection symmetry with respect to a {110} plane can couple together to make four pair bonds, leaving two dangling bonds at the A and B atoms. These two dangling bonds separated by four vacancies interact with each other to give rise to a spin-1 spectrum. The zero-field splitting, estimated in terms of the magnetic dipole-dipole interaction, is in good agreement with the experimental value.[11]

We performed a quenching experiment with the external ⟨110⟩ stress of 2250 kg/cm^2 at 140 °C. Details of the experimental procedure are the same as those described for the $P1$ center in Sec. III A. Figure 7 shows the spectrum taken at room temperature with $\vec{H} \parallel$ ⟨110⟩ (a) with zero stress and (b) with the quenched-in alignment. We know from Watkins and Corbett's work[3] that the divacancy is aligned in such a way that the compression stress pushes the pair-bonding atoms closer together so as to lower its orbital energy. If we apply their

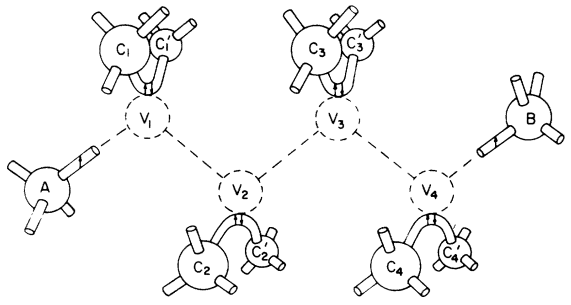

FIG. 6. {110}-planar tetravacancy chain (the $P3$ spectrum); two unpaired electrons are localized at the dangling bonds associated with the A and B atoms, respectively, giving rise to a spin-1 center, and the first-neighbor atoms form a pair-bonding orbital such as ($C_1 + C_1'$), ($C_2 + C_2'$), etc.

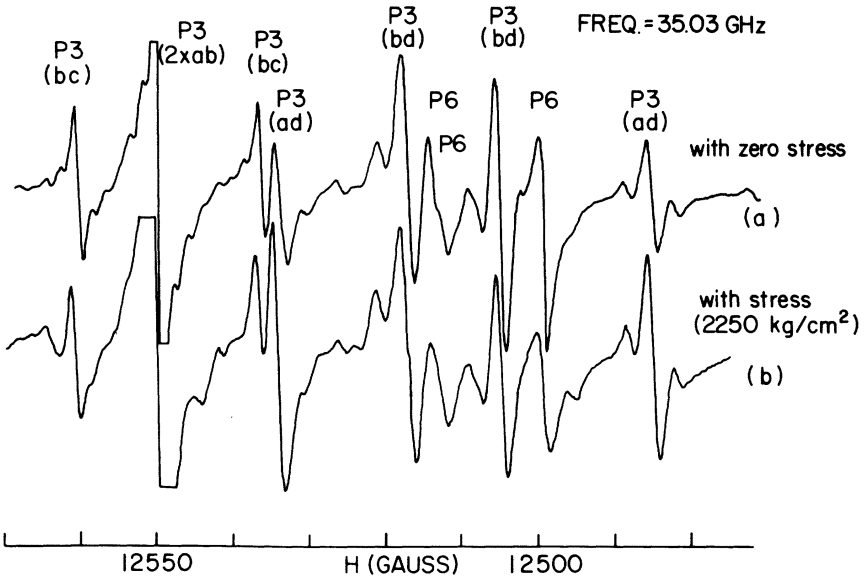

FIG. 7. $P3$ spectrum observed at 300 °K ($\vec{H} \| \langle 110 \rangle$): (a) as all the defect sites are degenerate; (b) after the degeneracy is lifted by the $\langle 110 \rangle$ stress and the preferential alignment is quenched from 140 °C to room temperature. Alignment shows that $N_{ad} > N_{bc}$ and $N_{ab} > N_{bd}$. $P6$ indicates the EPR lines of the $P6$ spectrum.

result to the planar tetravacancy chain, we should expect the alignment to be $N_{ad} > N_{ab} > N_{bd} > N_{bc}$, consistent with the present result shown in Fig. 7 (b).

In Sec. III A, we found that the reorientation of the defect axis through vacancy motion is a dominant effect in repopulation of the defects under the external stress; i.e., the defects are equally created first and then reach the thermal equilibrium in the deformed crystal, favoring a certain orientation. Therefore, a quantitative analysis can be carried out by using Eqs. (5), (6), and (8), and the results are given in Table II. It should be emphasized, however, that we did not take account of the loss of alignment which may have occurred while transferring the sample to the cavity.

Viewed from the defect structure which contains four pair bonds across each of four vacancies and parallel to the $\langle 110 \rangle$ axis of the $\{110\}$-reflection plane, we would anticipate the defect energy B_2 to be roughly a factor of 4 larger than what we estimated if we follow the argument by Watkins and Corbett that the divacancy center has a B_2 value twice as large [experimentally, $B_2 (= M) = 32$ eV/(unit strain)] as the phosphorus-plus-vacancy pair [$B_2 = 16$ eV/(unit strain)], because the former involves two pair bonds and the latter has only one. (Those values given here were calculated on the assumption that $B_1 = B_3 = B_4 = 0$.) However, if the defect energy B_2 is mainly associated with the internal strain created around the vacancies, as pointed out by Phillips,[14] the additivity of the energy may not hold when a large number of vacancies are involved. But B_2 should be the largest among the components of the B tensor, in any event consistent with the present result.

A positive value for both B_2 and B_4 strongly indicates that the $P3$ defect should be a $\{110\}$-planar vacancy chain rather than any vacancy cluster. We may expect a small negative value of B_1 for the $P3$ center, because the two atoms at the ends of the vacancy string would move away from each other as the pair-bonding atoms approach to each other. The two remote atoms, where the two resonant electrons are localized, are obviously coupled by the "extended" bonding orbitals, but the bonding should be very weak so as to form a triplet state and a small B_1 is expected. We conclude therefore that our stress results confirm the defect model of the $\{110\}$-planar tetravacancy chain as being responsible for the $P3$ spectrum.

C. Other spectra

We have reported the EPR spectra, $A1$, $A2$, $\cdots$, $A7$, identified in high-fluence (10^{18} n/cm^2) neutron-irradiated silicon, and some of these paramagnetic centers were discussed in terms of their tentative models.[12] Although stress alignment at a high temperature was observed in some of the centers we do not attempt here to calculate the piezospectroscopic tensor (the B matrix), because measurement of the relative intensity already involves a significant error owing to a considerable superposition in the lines. In Table I, we present the degree of alignment, $n_\perp / n_\parallel$, for the spectra where the alignment was clearly measured.

As discussed in detail in Ref. 9 the g shift suggests the structure of the resonant orbital as well as the charge state of a spectrum; if $\Delta g_\parallel \simeq 0$ and $\Delta g_\perp > 0$, the spectrum arises from a negative charge state of a broken bond or of parallel pair bonds; if $\Delta g_\parallel \simeq 0$ and $\Delta g_\perp \lesssim 0$, the spectrum is due to a positive charge state of a broken bond or parallel pair

bond; if $\Delta g_{\parallel} > 0$ and $\Delta g_{\perp} > 0$, the resonance occurs in a bent pair bond. Also, the symmetry of the g tensor reflects the local symmetry around a defect. Based on this additional information, we will discuss a tentative model for each spectrum.

1. Si-$A3$

The $A2$ and $A3$ spectra show the ⟨111⟩-axial symmetric g tensor (i.e., trigonal symmetry), and their g shifts suggest that the $A2$ spectrum would arise from a positive charge state, while the $A3$ is from a negative charge state. The behavior of the two centers is very close to each other; i.e., they appear simultaneously at 170 °C, where the {110}-planar tetravacancy chain ($P3$) disappears, and then $A2$ disappears at the 300 °C anneal and $A3$ at 350 °C. The degree of alignment $(n_{\perp}/n_{\parallel})$ is 0.71 and 0.65 for $A2$ and $A3$, respectively. We did not see a line-narrowing effect due to electronic motion in either spectra. In both spectra, we have resolved the Si^{29} hyperfine structure which corresponds to one equivalent atomic site.

The smallest {111}-planar vacancy cluster is made of four vacancies, V_1, V_2, V_3, and V_4, as shown in Fig. 8 (a). The local symmetry around the defect is trigonal (C_{3v}) and its threefold rotational axis is aligned in the ⟨111⟩ crystal axis parallel to the dangling bond A. A simple one-electron linear-combination-of-atomic-orbitals–molecular-orbitals (LCAO-MO) treatment predicts the electronic structure presented in Fig. 8 (b), in terms of the dangling-bond orbitals attached to each atom in the vicinity of the vacancy cluster. In the singly negative charge state, the unpaired spin is localized in the A orbital associated with the A atom, but it sits in the orbital $B+C+D$ in the singly positive charge state. Since both charge states belong to the A_1 representation in the C_{3v} group, no Jahn-Teller distortion is expected, as is consistent with the temperature independence of the g tensor; i.e., the orbital A or $B+C+D$ gives rise to an ⟨111⟩ axially symmetric g tensor. The Si^{29} hyperfine structure of the $A3$ spectrum is also consistent with the prediction for the singly negative charge state. But in the singly positive charge state, we anticipate the hyperfine interaction corresponding to three equivalent sites, contradicting what we found in the $A2$ spectrum. Also, there are three pair-bonding orbitals, $B+B''$, $C'+C''$, and $D+D''$, which are mainly affected in the stress alignment, because we know from Eqs. (4) that a trigonally symmetric defect involves only two components of the piezospectroscopic tensor (B_1 and B_2). Since only $C'+C''$ is parallel to the g_2 axis, the stress response to an external ⟨110⟩ stress will largely depend on the B_1 component (due to the other two orbitals) and the degree of alignment $(n_{\perp}/n_{\parallel})$ will be less than 1, consistent with the stress result we obtained in the $A3$ spectrum. Thus, our experimental results favor this model being attributed to the $A3$ spectrum. Presumably, the {111}-planar tetravacancy cluster would be energetically more stable than the {110}-planar tetravacancy center (the $P3$ spectrum) and vacancy motion at a high temperature will readily convert the {110}-planar defect ($P3$) into the cluster ($A3$)—it requires a vacancy to make three successive jumps. This clustering process must occur at ~170 °C, where the $A3$ spectrum appears along with diminution of the $P3$ spectrum. Therefore, we tentatively conclude that the singly negative charge state of the {111}-planar tetravacancy cluster gives rise to the $A3$ spectrum. The $A2$ spectrum appears to arise from a nonplanar vacancy cluster but requires more study to identify a defect.

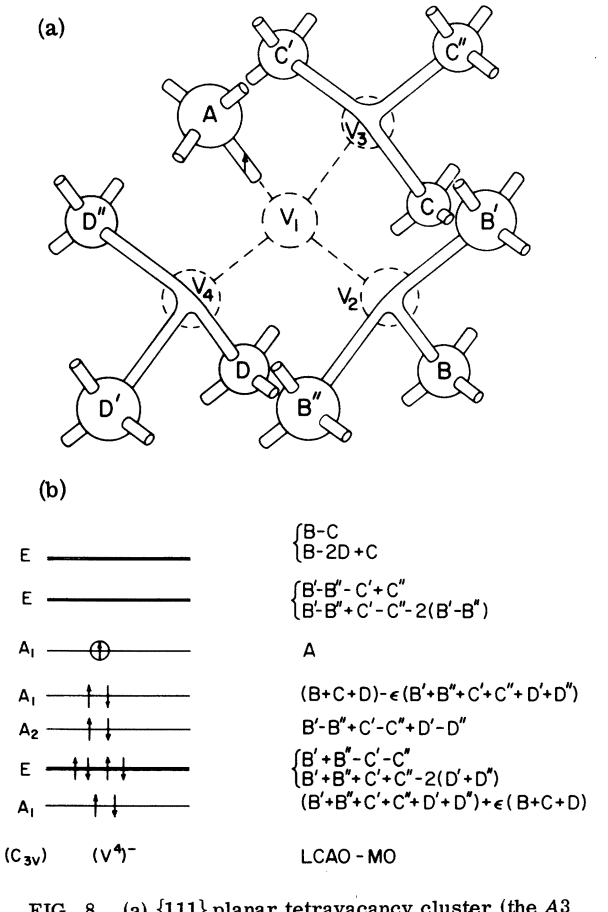

FIG. 8. (a) {111} planar tetravacancy cluster (the $A3$ spectrum); three vacancies V_2, V_3, and V_4 in an {111} plane and V_1 is in another {111} plane apart from the former by $\frac{1}{3}$ of the Si–Si bond distance, so that the four vacancies form a trigonal pyramid. (b) Simple LCAO-MO prediction of the electronic structure, where mixing between the orbitals in the same representation was allowed among the first-neighbor atoms.

2. Si-$A4$

The $A4$ spectrum can be observed in the annealing temperature range 100–250 °C. The symmetry of the g tensor suggests that the resonant electron is localized in the "bent-pair"-bonding orbital extended over an odd number of vacancies in the ⟨110⟩ direction. Since a single vacancy is mobile at room temperature, the number of vacancies should be more than 1. The degree of the quenched-in alignment under the ⟨110⟩ uniaxial stress is 1.40, which is the same sense as that of the $P3$ spectrum, the {110}- planar tetravacancy chain. We note that two opposite senses of defect alignment ($n_\perp/n_\parallel$ is 0.72 for $P1$ and 1.40 for $A4$) are observed in the two spectra which appear simultaneously in a single run of the experiment (225 °C annealing with 2200 kg/cm^2). This is clear evidence to support our view that the sense of quenched-in alignment is independent of the annealing behavior of a particular defect, but reflects the microscopic nature of the bonding orbitals around a defect. The stress result of $A4$ strongly suggests the model of a {110}-planar multiple-vacancy chain in the ⟨110⟩ direction. Since the {110}-planar tetravacancy center is unstable beyond the 170 °C anneal and the divacancy center ($G6$ and $G7$) is stable up to 350 °C, it is rather reasonable to believe that the trivacancy center may be responsible for the $A4$ spectrum. However, the pentavacancy center cannot be positively excluded as a candidate, because either of them satisfies the presently accumulated results on the $A4$ spectrum—the g tensor, the Si^{29} hyperfine structure, and the stress alignment.

Jung and Newell[10] first identified three oxygen-dependent spin-1 centers, $P2$, $P4$, and $P5$, in neutron-irradiated silicon, after heat treatment, and then Brower[11] argued that the $P2$ spectrum is attributed to the divacancy-plus-oxygen center and that both $P4$ and $P5$ spectra are due to the trivacancy-plus-oxygen centers with the oxygen atom being trapped at different vacancy sites. It is generally known that the oxygen impurity trapped in a vacancy site plays an important role in the stabilization of vacancy-associated defects. We note that the vacancy-plus-oxygen, the $B1$ spectrum, anneals near 350 °C but a single vacancy ($G1$ and $G2$ spectra) is unstable at ~ – 100 or – 200 °C, depending on its charge state.[16] However, the oxygen atom trapped in the divacancy ($P2$) does not strongly influence the defect energy as effectively as in the single-vacancy center, although they are in the same direction (i.e., the divacancy, $G6$ and $G7$, anneals at 350 °C but the divacancy-plus-oxygen at 400 °C). Botvin *et al.*[17] did observe both $P4$ and $P5$ spectra in proton- (or α-particle) bombarded silicon, but not the $P2$ spectrum, which can be easily seen in neutron irradiation. Based on the annealing data of $P4$ (450 °C) and of $P5$ (500 °C), we may anticipate that the trivacancy center would anneal out at a lower temperature than that of the $P4$ spectrum, and that it must be created in a considerable amount in float-zone silicon. Therefore, the $A4$ spectrum should be more likely to be a negative charge state of the trivacancy center. We should note, however, that those oxygen-dependent centers require more detailed studies to confirm the defect models.

Finally, it is interesting to note that the {110}-planar tetravacancy center anneals at 170 °C, the trivacancy $A4$ at 250 °C, and the divacancy at 350 °C, but the nonplanar pentavacancy cluster $P1$ is stable at much higher temperature (~ 450 °C). This is the first indication in the EPR studies that the {110}-planar multiple-vacancy chain is relatively unstable and that it eventually evolves to more stable vacancy agglomerates through a clustering process, while annealing.

IV. SUMMARY AND CONCLUSION

Rigorous treatment of the uniaxial-stress effect is made in terms of the Kaplyanskii piezospectroscopic tensor. These results are compared with the previous equations developed by Watkins and Corbett for the analysis of stress effects in the radiation-induced defects. Particularly, we have found that there exists differences in stress alignment between the C_{2v}-symmetric (rhombic I) defects and the C_{1h}-symmetric (monoclinic I) ones. This approach is used to analyze the experimental results of the $P1$ and $P3$ spectra. Based on the quenched-in alignment among equivalent defect sites, we have confirmed that the $P1$-spectrum arises from a negative charge state of the nonplanar pentavacancy cluster, and that the $P3$ spectrum is due to a neutral charge state (spin 1) of the {110}-planar tetravacancy chain. Also, tentative models of the $A3$ and $A4$ spectra are constructed; the $A3$ is attributed to a negative charge state of the {111}-planar tetravacancy cluster and the $A4$ spectrum to a negative charge state of the trivacancy center.

In light of the annealing behavior of those well-understood defects, we conclude that {110}-planar vacancy chains are relatively unstable and tend to form nonplanar vacancy clusters as temperature increases.

ACKNOWLEDGMENTS

We wish to express our appreciation to Dr. John Cleland (Oak Ridge National Laboratory) for his aid in the neutron irradiations, to Dr. G. D. Watkins for helpful conversations, and to the Dow, Corning, and Monsanto companies for supplying the samples.

*Research reported in this paper was supported in part by the Office of Naval Research under Contract No. N00014-70-C-0296.

[1]G. D. Watkins and J. W. Corbett, Phys. Rev. 121, 1001 (1961).
[2]G. D. Watkins and J. W. Corbett, Phys. Rev. 134, A1359 (1964).
[3]G. D. Watkins and J. W. Corbett, Phys. Rev. 138, A543 (1965).
[4]The {110}-symmetric defect means the one that contains the reflection symmetry in the {110} plane.
[5]A. A. Kaplyanskii, Opt. Spectrosc. 16, 329 (1964).
[6]W. Voigt, *Lehrbuch der Kristallphysik* (Tuebner, Leipzig, 1966), p. 593.
[7]E. L. Elkin and G. D. Watkins, Phys. Rev. 174, 88 (1968).
[8]M. Nisenoff and H. Y. Fan, Phys. Rev. 128, 1605 (1962).
[9]Y. H. Lee and J. W. Corbett, Phys. Rev. B 8, 2810 (1973).
[10]W. Jung and G. S. Newell, Phys. Rev. 132, 648 (1963).
[11]K. L. Brower, Radiat. Eff. 8, 213 (1971).
[12]Y. H. Lee, Y. M. Kim, and J. W. Corbett, Radiat. Eff. 15, 77 (1972).
[13]K. L. Brower, F. L. Vook, and J. A. Borders, Appl. Phys. Lett. 15, 208 (1969).
[14]J. C. Phillips, Comments Solid State Phys. 3, 67 (1970).
[15]G. D. Watkins, Phys. Rev. 155, 802 (1967).
[16]J. W. Corbett, *Electron Radiation Damage in Semiconductors and Metals* (Solid State Phys. Suppl. 7) (Academic, New York, 1966).
[17]V. A. Botvin, Yu. V. Gorelkinskii, V. O. Sigle, and M. A. Chubisov, Sov. Phys.-Semicond. 6, 1453 (1973).